Supporting Information

Extended Experimental Procedures
Supporting Figures
Supporting Dataset

Isomer-specific effect of microRNA miR-29b on nuclear morphology

Alison J. Kriegel[1,*], Scott S. Terhune[2,3], Andrew S. Greene[1,3], Kathleen R. Noon[3], Michael S. Pereckas[3], and Mingyu Liang[1,*]

From the [1]Department of Physiology, Center of Systems Molecular Medicine, [2]Department of Microbiology and Molecular Genetics, and [3]Biotechnology and Bioengineering Center, Medical College of Wisconsin, Milwaukee, Wisconsin 53226

Running title: *Isomer-specific effect of miR-29b*

*To whom correspondence should be addressed : Mingyu Liang, M.B., Ph.D : Department of Physiology, Medical College of Wisconsin, mliang@mcw.edu, Tel: 1-414-955-8539, Fax: 1-414-955-6546 or Alison J. Kriegel, Ph.D.: Department of Physiology, Medical College of Wisconsin, akriegel@mcw.edu, Tel: 1-414-955-4835, Fax: 1-414-955-6546

Extended Materials and Methods

Biotinylated miRNA duplexes

Oligonucleotide sequences mimicking miR-29b, miR-29a, or scrambled miR-29b with a biotin tag at the 3' end, and an unbiotinylated miR-29b (Supporting Figure 1) were synthesized by Dharmacon. The duplex strands were annealed by heating at 60°C for 5 min, pulse centrifugation and 30 minutes of cooling at room temperature.

Cell culture, RNA extraction and qPCR

HeLa cells were cultured in high glucose DMEM (Invitrogen) with 10% fetal bovine serum (Sigma). RNA was extracted using the Trizol method and quantitative real-time PCR (qPCR) analysis of collagen family members was performed as previously described (*2,3*). Primer sequences used were (5' to 3') Col1a2 fw AACAACCAGATTGAGACCCTTCTTACT, rv GGGTGGCTGAGTCTCAAGTCA; Col2a1 fw GCAGAGGGCAATAGCAGGTT; rv GATAACAGTCTTGCCCCACTTACC; Col3a1 fw GCTGTGAGACTACCTATTGTAGATATTGC, rv TTGGGATTTCAGATAGAGTTTGGTT; Col4a1 fw CCATTTCCGTGGTTTCTCATG, rv GGCCTAGTGGTCCGAATCTG. Expression of miR-29a and miR-29b was measured by qPCR using TaqMan miRNA assays (Life Technologies), and normalized to 5s rRNA expression, as previously described (*2,3*).

Affinity purification of miRNA-specific miRNPs and proteomic analysis

HeLa cells at 70% confluence in 10 cm dishes were transfected with biotinylated miR-29a, miR-29b, or scrambled miR-29b or unbiotinylated miR-29b mimetic oligonucleotide duplexes at a final concentration of 133 nM using Lipofectamine 2000 (Invitrogen) (n=3 per group). Medium was replaced after 5 hours. Cells were collected 48 hours later and centrifuged at 400 x g for 10 minutes. The cells were resuspended in 200 uL of lysis buffer A [10 mM Tris (pH 8.0), 140 mM NaCl, 1.5 mM MgCl2, 0.5% Nonidet P-40]. Cells were incubated on ice for 5 minutes, followed by a 3 minute 1,000 x g centrifugation at 4° C (*7*). The supernatant from the resulting fractionation was frozen in liquid nitrogen. The pelleted fraction was rinsed twice with lysis buffer A, followed by a third rinse in lysis buffer A with 1% Tween-40 and 0.5% deoxycholic acid. The pellet was resuspended in 20 µL of PVP buffer (20mM Hepes/1.2% PVP with 1:100 protease inhibitor), frozen in liquid nitrogen as spherical pellets (*4,5*), and pulverized by 6 cycles of cryogenic grinding on a TissueLyser (Qiagen) at 30 Hz for 1 minute.

The resulting powder and the frozen supernatant fraction from each plate of cells were resuspended in 1 mL of lysis buffer (20 mM K-HEPES, pH 7.4, 110 mM potassium acetate, 2 mM $MgCl_2$, 0.1% v/v Tween 20, 1 µM $ZnCl_2$, 1 µM $CaCl_2$, 0.255 Triton, 150 mM NaCl, 1:100 v/v protease inhibitor) and cellular debris was removed by centrifugation at 400 x g for 10 minutes at 4ºC. The supernatant from each fraction was incubated with 0.8 mg of streptavidin coated magnetic Dynabeads (Life Technologies) on a rotor at 4ºC for 3 hrs. Streptavadin coated dynabeads were isolated by magnets and washed in lysis buffer 6 times. Isolated proteins were eluted (0.5N NH4OH, 0.5mM EDTA) over 20 minutes on a Tomy shaker and dried down by speed vacuum.

Proteins were resuspended in 20uL of homogenization buffer (20mM HEPES pH 7.5, 1mM EDTA, 1:100 protease inhibitor) and 20 uL of Lamelli buffer (with beta-mercaptoethanol) and run out ¼ of the length of a 10% SDS-PAGE gel (Bio-Rad). The gel was fixed in 10% acetic acid, 16% MeOH, rinsed and stained using coomassie blue. Proteins from each sample were excised

from the gel in two equally sized sub-fractions which were minced. Destaining of the gel fragments was performed with several washes of 40% MeOH, 7% acetic acid (v/v). Proteins were reduced with 10mM DTT in 50mM ammonium bicarbonate for 30 minutes at 37 °C with mixing. Cysteines were alkylated with 55mM iodoacetamide in 50mM ammonium bicarbonate for 45 minutes at 37 °C in the dark, with mixing. Gel pieces were washed to remove excess reagents then dried in a vacuum centrifuge. One microgram of trypsin was added to each gel piece and the samples were incubated overnight at 37 °C with mixing. Peptides were extracted for 20 minutes at 37 °C with three solutions: 1) 0.1% TFA in water (v/v); 2) 70% ACN: 0.1% TFA in water (v/v); and 3) 90% ACN: 0.1% TFA in water (v/v). The supernatants were pooled with the original digest solution then dried in a vacuum centrifuge. Dry extracts were dissolved in 20µL 0.1% TFA in water (v/v), mixed briefly, sonicated for 20 minutes, then centrifuged at 21,000 xg for 5 minutes. Samples were desalted with C18 ZipTips (0.6µL resin, Millipore Corporation, Billerica, MA), and eluted from the ZipTips with 3 aliquots of 70% ACN: 0.1% TFA in water (v/v). The combined eluates were dried in a vacuum centrifuge and stored at -20 °C. Just prior to LC-MS/MS analysis, the dried samples were reconstituted in 8µL 95% water:5% ACN:0.1% formic acid (v/v/v), mixed briefly, sonicated for 20 minutes, then centrifuged at 21,000xg for 5 minutes to remove any insoluble material.

Samples were analyzed in duplicate by liquid chromatography-tandem mass spectrometry (LC-MS/MS) using a Surveyor NanoLC interfaced to an LTQ linear ion trap mass spectrometer with nanoelectrospray ionization (Thermo Scientific). Peptides were chromatographically separated with a reverse phase column of dimensions 10cm x 75µm I.D. packed in house with Magic C18 300A 5µm particles (Michrom Bioresources) using a binary gradient. Solvent A was 95% water: 5% acetonitrile: 0.1% formic acid (v/v/v) and Solvent B was 5% water: 95% acetonitrile: 0.1% formic acid (v/v/v). Flow through the column was approximately 400 nL/minute and the peptides were separated with a linear gradient from 5% Solvent B to 75% Solvent B over 180 minutes. Positive ions were generated with a spray voltage of 1.8 kV. Mass spectrometric data were collected in data-dependent mode with MS/MS spectra recorded on the six most abundant ions in the survey scan and dynamic exclusion enabled. The normalized collision energy was set to 35%. Xcalibur software (Thermo Scientific) was used for instrument control and data acquisition. In total, 8 runs of LC-MS/MS analysis were performed for each biological replicate sample.

Visualize software, designed by Dr. Brian Halligan at the Medical College of Wisconsin (open access, www.BBC.mcw.edu), was used to evaluate and analyze the proteomic data. Protein hits from all fractions in each biological sample were combined, resulting in a single list of proteins purified from each original plate of transfected cells. The protein lists from all three biological replicates from each of the experimental controls (biotinylated scrambled miR-29b and unlabeled miR-29b) were combined to generate a list of nonspecifically purified contaminant proteins. Proteins were considered to be present, if they had been identified with a probability greater than 0.85, at least two peptides were observed and they were detected at least twice in this combined list. The entire list of all contaminating proteins was subtracted from the list of proteins identified from each of the biological triplicates from the experimental samples to identify miR-29b or miR-29a interacting proteins. We then applied the exclusionary thresholds to the resulting lists of specific miRNA duplex interacting proteins (protein probability >0.85, peptide count $\geq$ 2, scan count $\geq$ 2) to minimize false discovery. The remaining proteins that were present in $\geq$2 out of the 3 biological replicates were included in our final lists of identified proteins. By comparing the

lists of miR-29b and miR-29a interacting proteins resulting from our stringent criteria for inclusion, we categorized identified proteins as miR-29b-specific, miR-29a-specific, or common to both miR29a and miR-29b (Supportingl Dataset).

Western blots

For EIF2C2 and ANT2 Western blots, cells were suspended in polyvinylpyrrolidone (PVP) buffer. Prior to affinity purification, 1/3 of each sample of whole cell lysate was saved. Western blots were performed as previously described (*2,3*) using antibodies for EIF2C2 (Santa Cruz) and ANT2 (AbCam). A single membrane was stripped (47 mM Tris-HCl pH 6.7, 15% v/v 10% SDS, 0.7% v/v β-mercaptoethanol for 30 min at 50°C) and re-blotted to obtain both Western blots.

Immunoprecipitation of ANT2-miRNA complexes

HeLa cells harvested at confluence were cryogenically ground as described in the affinity purification protocol. Cells were lysed in lysis buffer and cleared of debris. The cell lysate was pre-cleared in Dynabeads Protein A for one hour while separate portions of the beads were incubated with ANT2 rabbit IgG antibody or IgG isotype control. The beads coated with anti-ANT2 or control IgG were rinsed with lyisis buffer and added to the pre-cleared cell lysate (n=3/group). Following a one hour incubation, the beads were rinsed as described above, and Trizol was added directly to the beads for RNA extraction.

In situ hybridization (ISH) and Immunocytochemistry (ICC)

At indicated time points, cells were rinsed with PBS and fixed in 10% formalin. ISH was performed as previously described (*6*). The 5' digoxigenin labeled miR-29b, miR-29a and miR-21 probes (Exiqon), as well as positive (U6, snRNA) and negative controls (scrambled), were hybridized overnight at 51°C. Cells were then incubated with a fluorescein labeled anti-digoxigenin antibody (1:100, Roche) followed by an Alexa 488 anti-fluorescein antibody to detect the miRNA probes. ICC was performed simultaneously with primary antibodies to either ANT2 (1:100, Abcam), EIF2C2 (1:100, Santa Cruz Biotechnology) or γ-tubulin (1:100, Abcam), followed by secondary antibodies (1:100 Texas red labeled goat anti-rabbit and 1:100 Texas red labeled goat anti-mouse, respectively). Coverslips were mounted in vectasheild containing DAPI for visualization of nuclei. All images were acquired using a Nikon A1-R laser scanning confocal microscope.

Knockdown of miR-29 and ANT2

HeLa cells at 30% confluency underwent a double block in 2 mM thymidine, as previously described (*7*). Following the first release (17 hours) cells were transfected with "in vitro" power inhibitors (anti-miR-scramble, anti-miR-29b or anti-miR-29a) (Exiqon) at a 133 nM final concentration, or siRNA (control siRNA, siEIF2C2 or one of two different siANT2; Life Technologies) at a 40 nM final concentration using Lipofectamine 2000 (Life Technologies) (*8,9*). Medium was replaced 5 hours later and the cells were blocked in thymidine for 14 hours, with release into 100 μM nocodazole where indicated.

Statistical Analysis

Data were analyzed using the Student's t-test and multiple-group analysis of variance (ANOVA). $P<0.05$ was considered significant. Criteria used for analyzing proteomic data are described in above. Data are shown as mean ± SEM.

SUPPORTING DATASET (See separate tabular Excel file)

Proteins interacting with miR-29a, miR-29b, or both. The dataset contains three sections. The first section shows proteins identified as interacting with miR-29b, but not miR-29a. The second section shows proteins interacting with miR-29a, but not miR-29b. The third section shows proteins interacting with both miR-29b and miR-29a. The identified proteins are shown with links to Uniprot (http://www.uniprot.org) and the KEGG (http://www.genome.jp/kegg) pathways they fall within. See Materials and Methods for detail of the proteomic analysis and criteria for protein identification and categorization.

SUPPORTING FIGURES

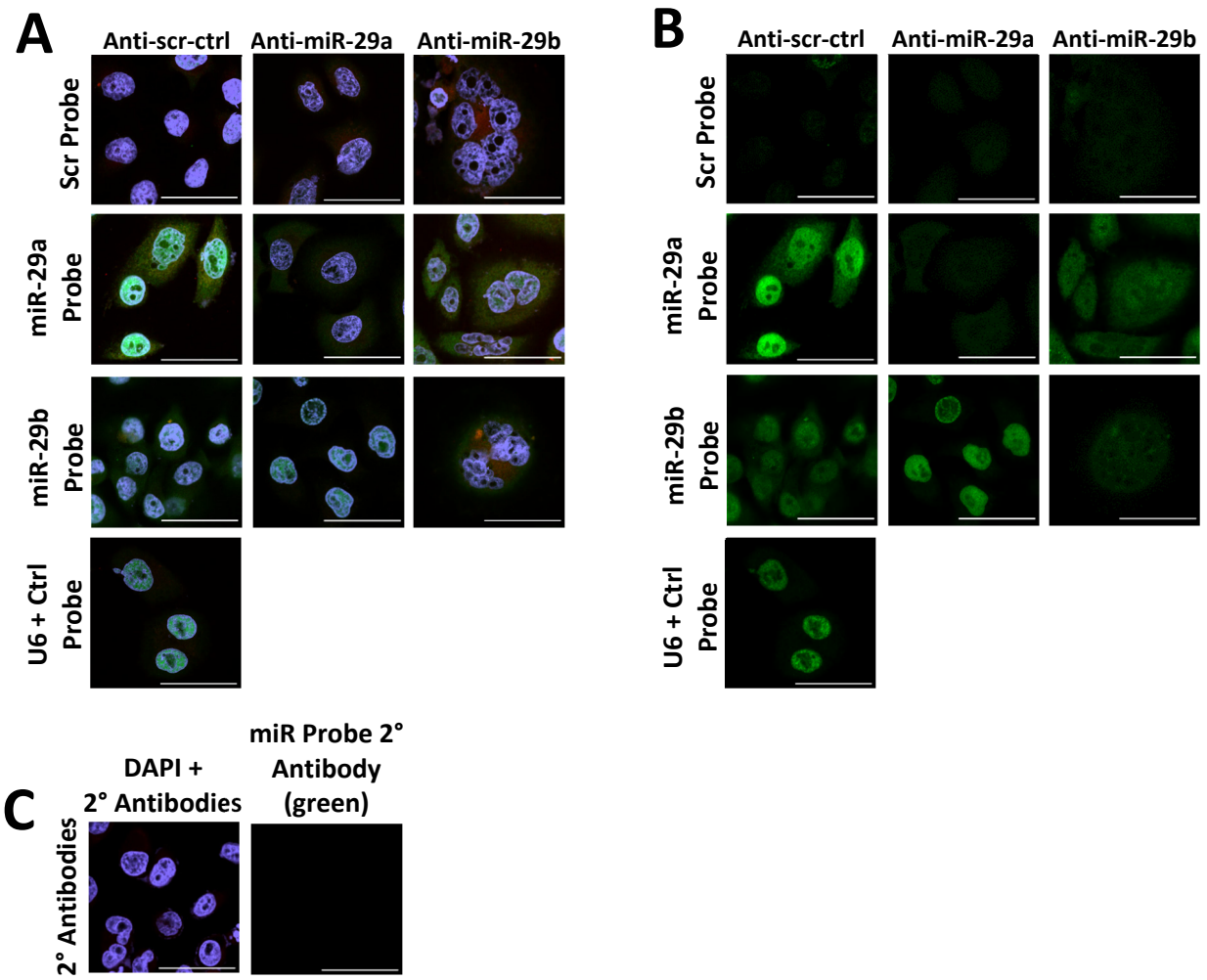

Supporting Fig. 1. miRNA in situ hybridization controls. *In situ* hybridization was performed 48 hours after HeLa were transfected with anti-scr-ctrl, anti-miR-29a or anti-miR-29b oligonucleotides to confirm the specificity of scrambled/ctrl, miR-29a and miR-29b inhibitors and probes. A) In situ hybridization and immunohistochemistry were performed for the indicated miR (green) and ANT2 (red), respectively. The nuclei were DAPI stained (blue). A probe for U6 nuclear RNA was used as a hybridization control. The in situ hybridization (miRNA-specific) signal has been isolated in panel B. The nuclear/cytoplasmic ratios for these miRNAs in HeLa cells are miR-29b= 2.44, miR-29a= 0.72, and miR-21= 0.47, as reported by Hwang, et al (*7*). Liao et al. (10) also reported that many microRNAs are found in the nuclear fraction of cells to some extent, while some miRNAs mostly in the cytoplasm. Our ISH results are consistent with these reports in that the miRNA signal coming from the nuclei is markedly stronger for miR-29b than miR-29a followed by miR-29a. C) There was no signal detected when cells were incubated with secondary antibody alone. These results indicate that the antibodies that we have used to detect the probes do not bind to chromosomes or cytoplasmic material non-specifically. Calibration bars are 50 μm in length.

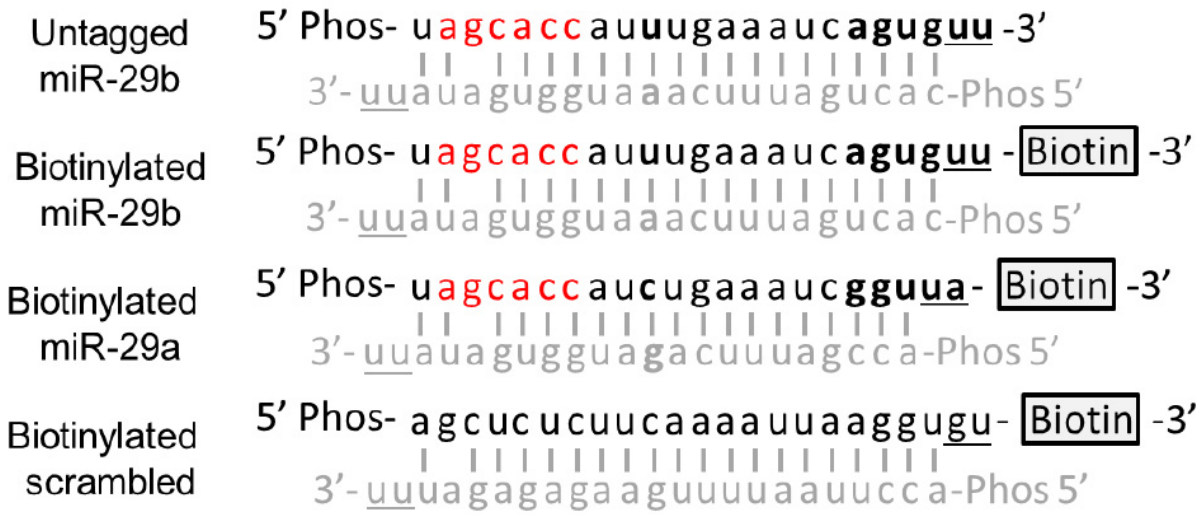

Supporting Fig. 2. Synthetic miRNA duplexes. The major strand sequences of each duplex are shown in black, with seed sequences in red, and the complementary sequences in gray. The sequence regions that differ between miR-29b and miR-29a are bolded. The 5' end was phosphorylated. The complementary sequences were designed such that, when duplexed, a 2 nucleotide overhang would exist on the 3' of each strand (underlined). Additionally, a mismatched nucleotide pairing (A/G) was introduced near the 5' end of each synthetic major strand to encourage dissociation of the duplex in cells (*14*).

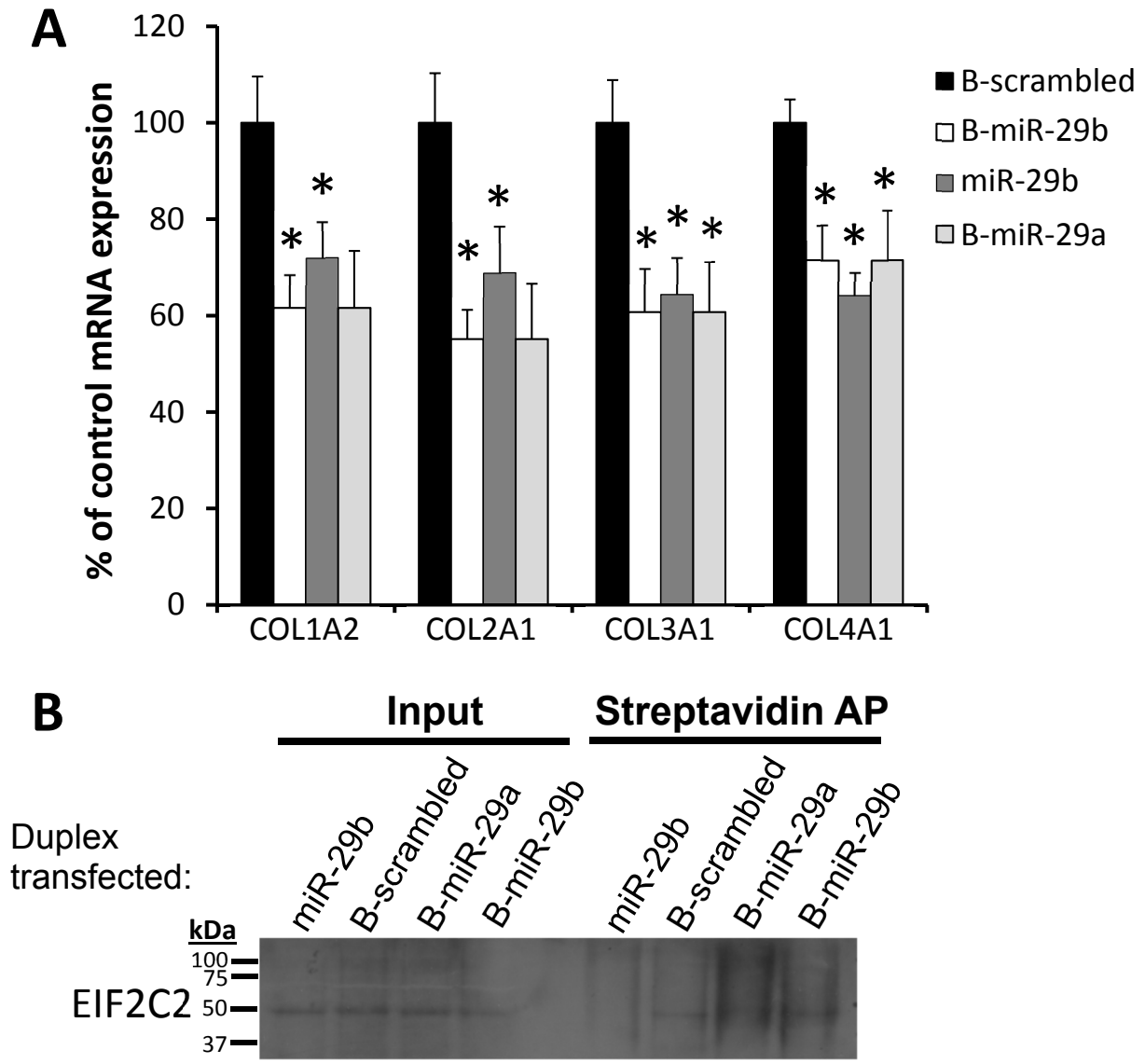

Supporting Fig. 3. Biotinylated synthetic miR-29b and miR-29a duplexes retained known functions of miR-29. A) Synthetic miR-29b duplexes with or without a biotin modification at the 3' end suppressed known miR-29 target genes *COL1A2*, *COL2A1*, *COL3A1 and COL4A1*. Biotinylated miR-29a also effectively suppressed these targets. N=8/group; *P< 0.05 vs biotinylated scrambled; ANOVA. B) EIF2C2 was detected by Western blot in protein samples affinity-purified (AP) from cells transfected with biotinylated-scrambled-miR, biotinylated miR-29a or biotinylated miR-29b, but not untagged miR-29b.

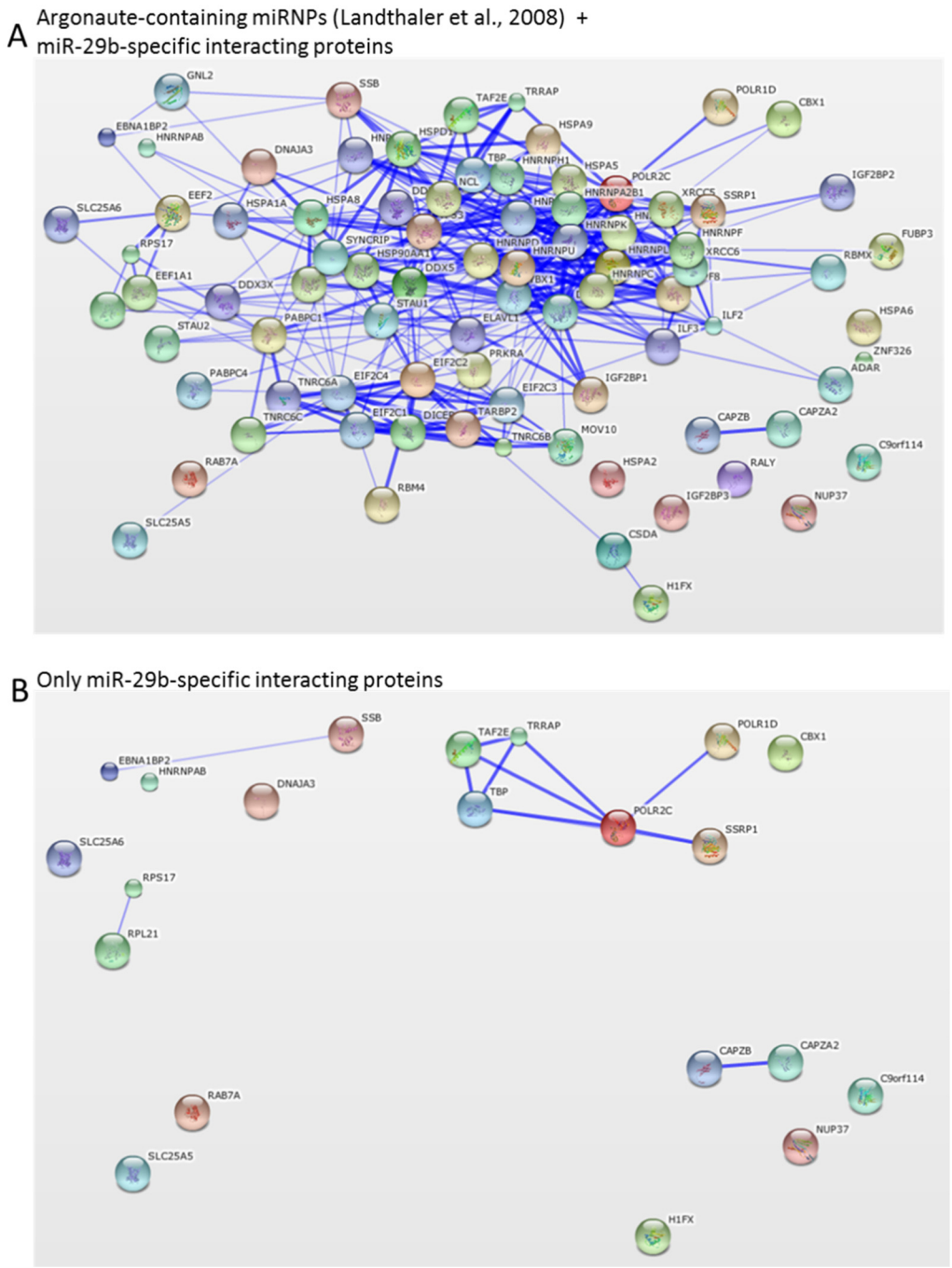

Supporting Fig. 4. **Associations of miR-29b-specific miRNPs in relationship to known argonaute-interacting proteins according to STRING database.** STRING includes direct and indirect protein-protein associations based on genomic context, protein-protein interaction experiments, and coexpression. A) Associations between all uniquely miR-29b interacting proteins identified in the present study and previously identified argonaute-interacting proteins (*11*). B) Associations of uniquely miR-29b interacting proteins alone [proteins identified only in Landthaler et al., 2008 (reference *11*) were removed].

A

Argonaute-containing miRNPs (Landthaler et al., 2008) +
miR-29a-specific interacting proteins

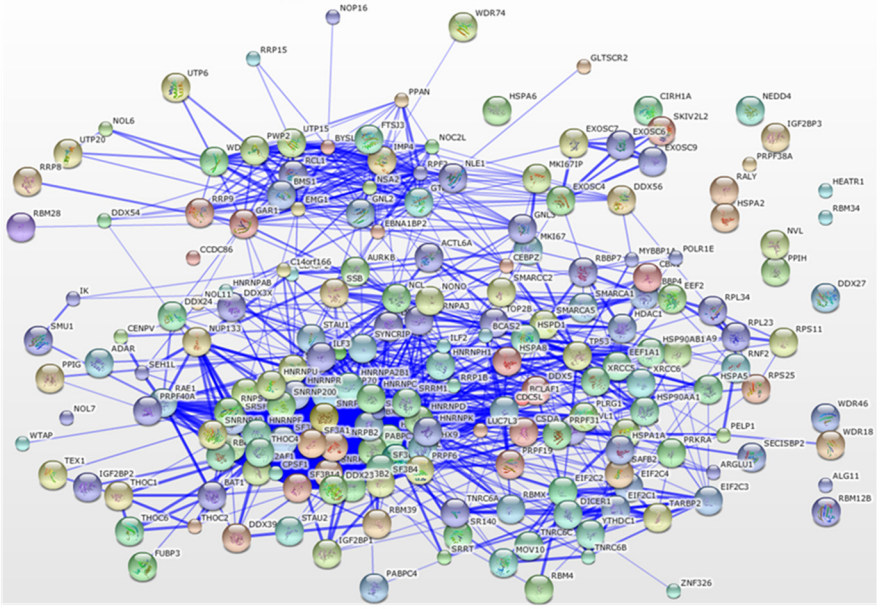

B

Only miR-29a-specific interacting proteins

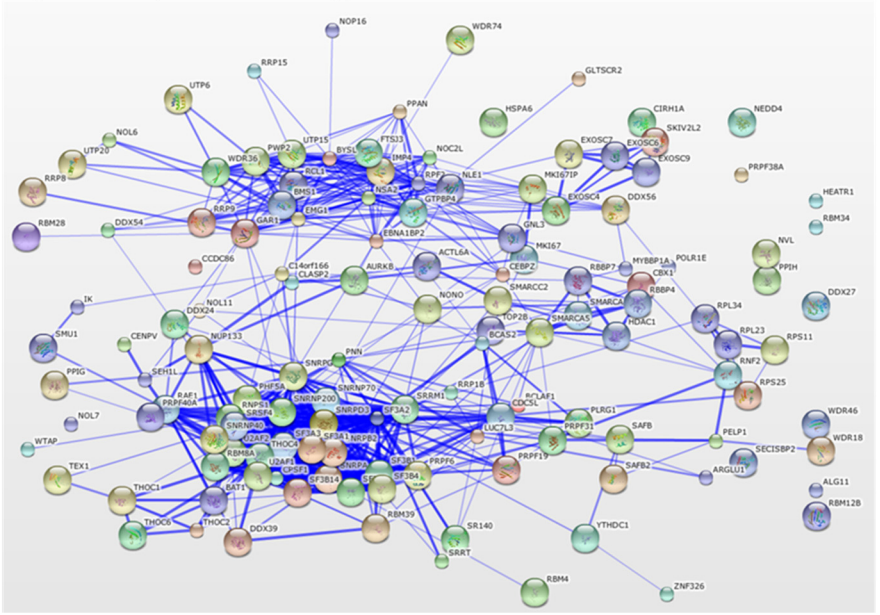

Supporting Fig. 5. Associations of miR-29a-specific miRNPs in relationship to known argonaute-interacting proteins according to STRING database. The analysis was similar to Supporting Fig. 4 except it focused on miR-29a-specific miRNPs.

A

Argonaute-containing miRNPs (Landthaler et al., 2008) +
miR-29a + miR-29b common interacting proteins

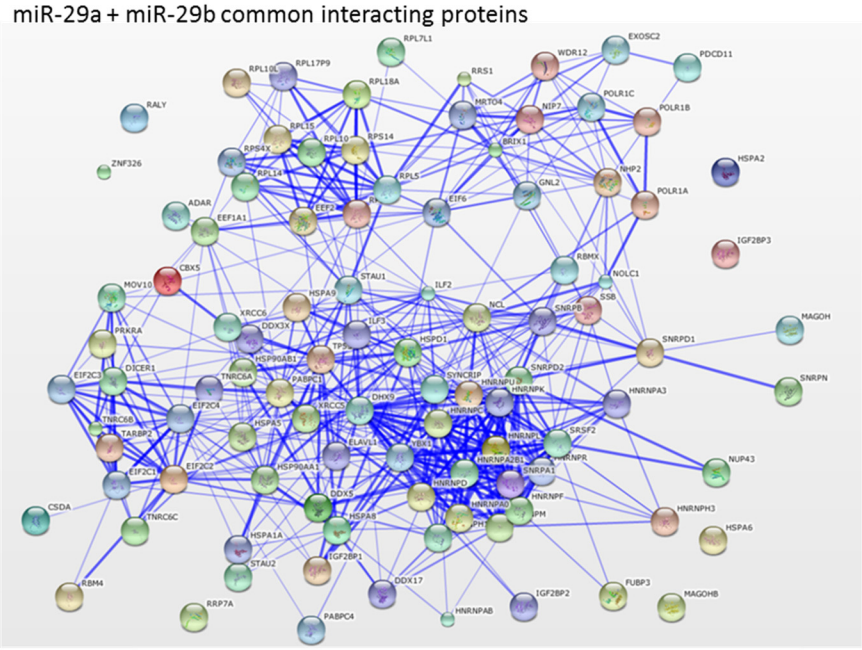

B

Only miR-29a and miR-29b common interacting proteins

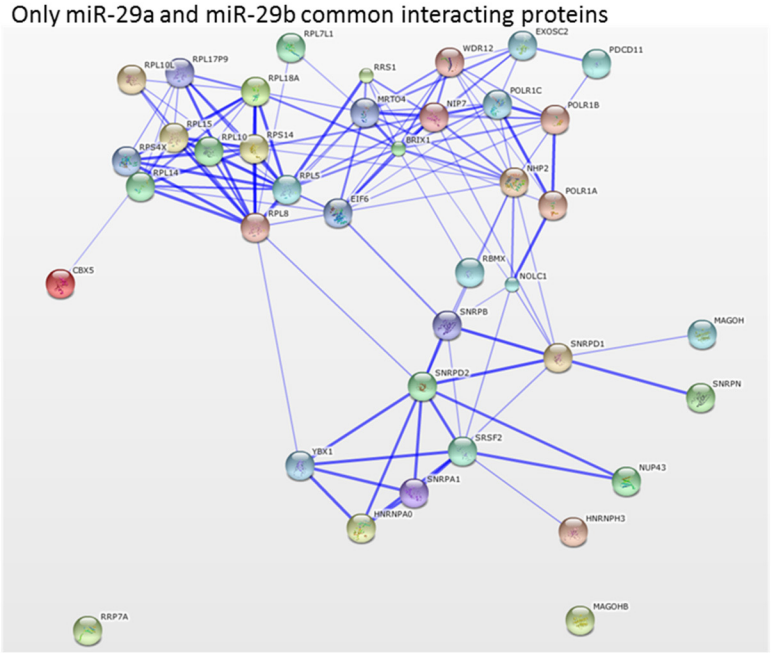

Supporting Fig. 6. Associations of miRNPs common to miR-29b and miR-29a in relationship to known argonaute-interacting proteins according to STRING database. The analysis was similar to Supporting Fig. 4 except it focused on miRNPs interacting with both miR-29b and miR-29a.

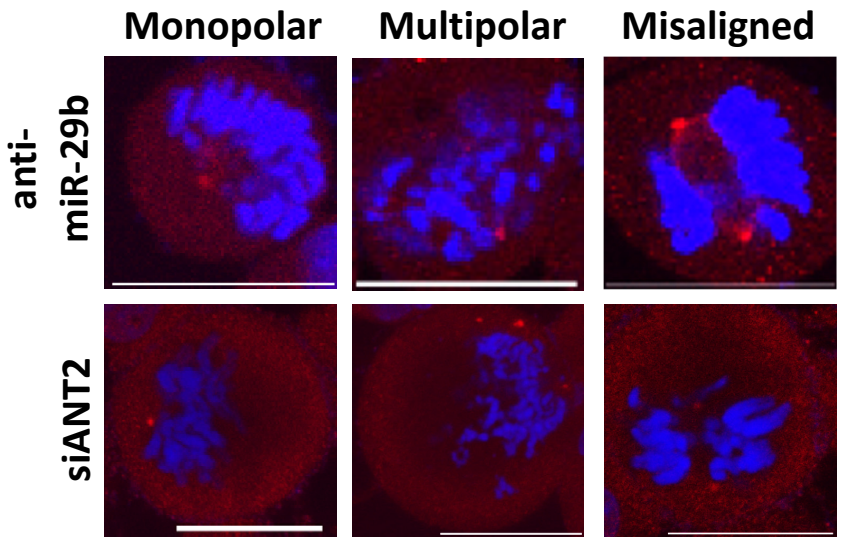

Supporting Fig. 7. Abnormal centrosome organization with miR-29b or ANT2 knockdown. Calibration bars are 25 μm in length.

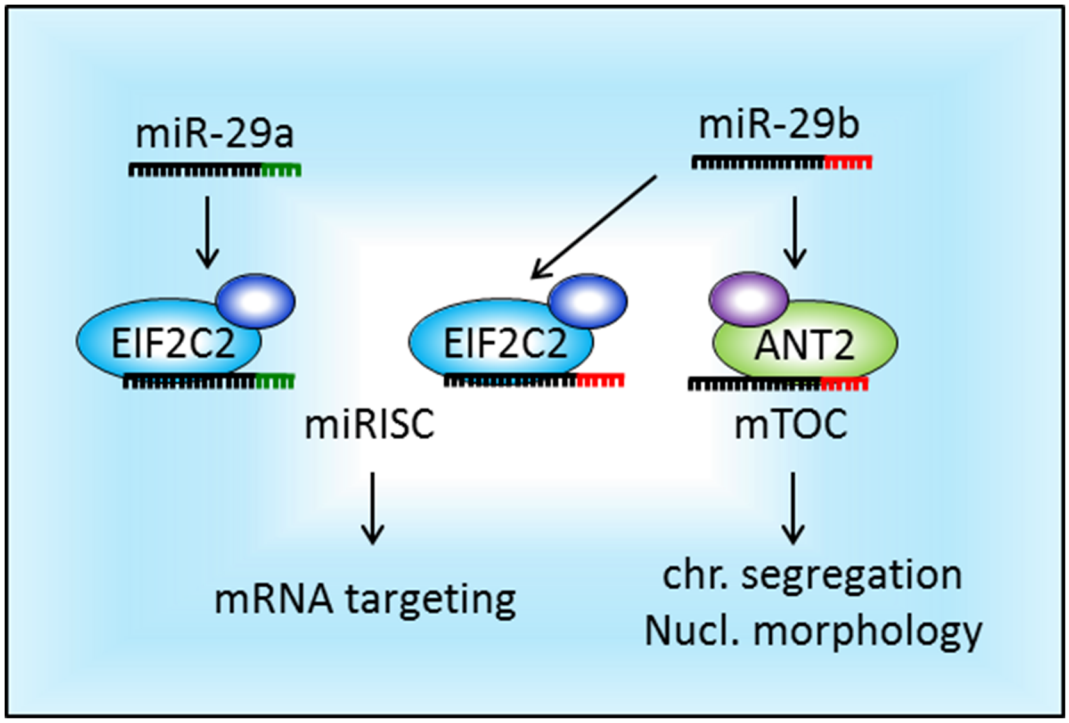

Supporting Fig. 8. Schematic diagram of conventional and unconventional mechanisms mediating biological effects of miR-29b. miR-29b, similar to miR-29a and other miRNAs, can target mRNAs via interaction with EIF2C2 and other microribonucleoproteins (miRNPs) in the miRNA-induced silencing complex (miRISC). However, miR-29b could regulate biological functions through unconventional mechanisms outside of miRISC and mRNA targeting. For example, miR-29b, but not miR-29a, contributes to normal chromosomal segregation and nuclear morphology via interaction with an unconventional miRNP, ADP/ATP translocase 2 (ANT2), at the microtubule-organizing center (mTOC).

miR-29a "in vitro" power inhibitor (20-mer): uagcaccaucugaaaucgguua
miR-29b "in vitro" power inhibitor (19-mer): uagcaccauugaaaucaguguu

Supporting Fig. 9. microRNA sequence regions targeted by miRCURY LNA™ microRNA Power Inhibitors (Exiqon) for miR-29a and miR-29b. The regions of miR-29a and miR-29b targeted by the respective RNA inhibitors are underlined in the miRNA sequences. The nucleotides differing in miR-29b vs. miR-29b are in bold. These inhibitors contain locked-nucleic acid modifications and a phosphorothioate backbone.

Supporting References

1. Landthaler, M., Gaidatzis, D., Rothballer, A., Chen, P.Y., Soll, S.J., Dinic, L., Ojo, T., Hafner, M., Zavolan, M., and Tuschl, T. Molecular characterization of human Argonaute-containing ribonucleoprotein complexes and their bound target mRNAs. *RNA*. **14**, 2580-2596 (2008).
2. Liu, Y., Taylor, N.E., Lu, L., Usa, K., Cowley, A.W. Jr, Ferreri, N.R., Yeo, N.C., and Liang, M. Renal medullary microRNAs in Dahl salt-sensitive rats: miR-29b regulates several collagens and related genes. *Hypertension*. **55**, 974-982 (2010).
3. Kriegel, A.J., Fang, Y., Liu, Y., Tian, Z., Mladinov, D., Matus, I.R., Ding, X., Greene, A.S., Liang, M. MicroRNA-target pairs in human renal epithelial cells treated with transforming growth factor beta1: a novel role of miR-382. *Nucleic Acids Res.* **38**, 8338–8347 (2010).
4. Moorman, N.J., Cristea, I.M., Terhune, S.S., Rout, M.P., Chait, B.T., and Shenk, T. Human cytomegalovirus protein UL38 inhibits host cell stress responses by antagonizing the tuberous sclerosis protein complex. *Cell Host Microbe* **3**, 253–262 (2008).
5. Cristea, I.M., Carroll, J.W., Rout, M.P., Rice, C.M., Chait, B.T., & MacDonald, M.R. Tracking and elucidating alphavirus-host protein interactions. *J Biol Chem* **281**, 30269–30278 (2006).
6. Kriegel, A.J., Liu, Y., Cohen, B., Usa, K., Liu, Y., and Liang, M. MiR-382 targeting of kallikrein 5 contributes to renal inner medullary interstitial fibrosis. *Physiol Genomics*. **44**, 259-267 (2012).
7. Hwang, H.W., Wentzel, E.A., and Mendell, J.T. A hexanucleotide element directs microRNA nuclear import. *Science*. **315**, 97-100 (2007).
8. Mladinov, D., Liu, Y., Mattson, D.L., Liang, M. MicroRNAs contribute to the maintenance of cell-type-specific physiological characteristics: miR-192 targets Na^+/K^+-ATPase β1. *Nucleic Acids Res.* **41**, 1273-83 (2013)
9. Tian, Z., Greene, A.S., Pietrusz, J.L., Matus, I.R., Liang, M. MicroRNA-target pairs in the rat kidney identified by microRNA microarray, proteomic, and bioinformatic analysis. *Genome Res.* **18**, 404-411 (2008)
10. Liao, J.Y., Ma, L.M., Guo, Y.H., Zhang, Y.C., Zhou, H., Shao, P., Chen, Y.Q., and Qu, L.H. Deep sequencing of human nuclear and cytoplasmic small RNAs reveals an unexpectedly complex subcellular distribution of miRNAs and tRNA 3' trailers. *PloS One*. **5**, e10563 (2010).